Research Square

Preprints are preliminary reports that have not undergone peer review.
They should not be considered conclusive, used to inform clinical practice,
or referenced by the media as validated information.

# Common Traits, Different Roles: Structural Position and Nonlinear Dynamics in Three-Party Bargaining

**George Lymperis**

geolib@rocketmail.com

University of Peloponnese

**Lambros B. Drossos**

University of Peloponnese

**Research Article**

**Keywords:** heterogeneous interacting agents, structural heterogeneity, bargaining dynamics, nonlinear dynamics, multistability, role assignment

**Posted Date:** September 19th, 2026

**DOI:** https://doi.org/10.21203/rs.3.rs-10962752/v1

**License:** This work is licensed under a Creative Commons Attribution 4.0 International License.
Read Full License

**Additional Declarations:** No competing interests reported.

# Common Traits, Different Roles: Structural Position and Nonlinear Dynamics in Three-Party Bargaining

**Abstract**

A familiar puzzle in negotiation is that the same parties, under the same institutional rules, can follow very different paths from different opening positions. This paper asks whether structural position—not actor traits alone—helps explain why. Three actors carry self-moderation, leverage, and vulnerability, while three bargaining roles determine how those traits enter local revision incentives. A local Nash revision game generates the continuous-time process, and an exact rescaling shows that only four combinations of the primitive coefficients govern its geometry. The model can settle, cycle, or remain irregular; most importantly, a stable settlement can coexist with another long-run path. That makes settlement accessibility an economic object: when opening positions are uncertain, the existence of a stable bargain does not tell us how easy it is to reach. In one benchmark, reassigning the same three trait bundles across roles more than doubles the share of plausible openings that settle. This role effect survives local perturbations of the nonlinear channels. Historical Phoenix data identify two government principal roles and a UNO third-party role and provide ordinal rankings of leverage, moderation, and vulnerability. The results show how institutional position changes bargaining dynamics by changing the channel through which fixed actor characteristics operate.

**Keywords:** heterogeneous interacting agents, structural heterogeneity, bargaining dynamics, nonlinear dynamics, multistability, role assignment

**JEL Classification:** C61 , C62 , C63 , C73 , D74

## 1 Introduction

Consider a wage negotiation involving a firm, a union, and a public mediator. The participants, their bargaining resources, and the institutional rules are fixed. In one meeting the opening positions are close enough that each subsequent revision makes the next difference smaller. The union moderates its demand, the firm softens its response, the mediator compromises, and bargaining settles. In another meeting the same participants begin the negotiation with their opening positions further apart. A

stronger demand triggers a harder response. The confrontation activates the mediator. The mediator's intervention changes the incentives of both parties and generates another round of repositioning. In both cases the participants remain the same and nothing about them is changed. Due to the different opening positions in the second case, however, the adjustment process can follow a different path and result in a different long-run state.

That example contains the question of this paper. Economic heterogeneity is usually attached to actors—their beliefs, preferences, capabilities, or adjustment rules (Brock and Hommes 1998; Hommes 2006). Bargaining institutions add another margin. Proposal rights affect outcomes (Baron and Ferejohn 1989); bargaining power depends on network position (Manea 2011; Abreu and Manea 2012); coercive capability changes counterpart incentives (Powell 1996); and third-party intervention is activated and transmitted through the configuration of the dispute (Kydd 2003; Rauchhaus 2006; Greig 2005). Here we ask what happens when the actors carry the same traits but those traits enter the bargaining process through different structural positions.

The mechanism is simple. The two principal positions respond directly to each other. A third position becomes active when their joint configuration activates it into play and then feeds back into both. Actors carry moderation, leverage, and vulnerability and roles determine the channels through which those traits operate. Therefore reassigning the same trait bundle can change the feedback process without changing the actor. Section 2 turns this idea into a model of reservation-relative bargaining stances and role-specific revision incentives.

We use continuous time to represent the evolution of stance between observed offers, threats, concessions, and interventions. A simultaneous short-horizon revision game supplies the strategic bridge: actors choose next stances while paying a cost for moving too abruptly, and the local Nash revision converges to the continuous adjustment law as revision opportunities become frequent. Continuous-time bargaining and frequent-revision models provide related precedents (Ambrus and Lu 2015; Ortner 2019), while negotiation-process work similarly treats observed actions as traces of an evolving process (Filzmoser et al. 2016).

The closest technical neighbors make the paper's point of departure sharper. Nonlinear economic games have long shown that strategic interaction can produce multistability, complex basin geometry, and endogenous periodic or chaotic dynamics (Agiza et al. 1999; Naimzada and Tramontana 2015; Bischi and Lamantia 2022). Three-group social and conflict models likewise generate oscillatory or chaotic trajectories (Kaufman et al. 2019; Nikolova and Vitanov 2020). In bargaining theory, informative outside options and third-party decisions can alter bargaining postures over repeated interaction (Lee and Liu 2013), and experimental evidence shows that strategically exposed third parties can transform conflict incentives (Halevy and Halali 2015). Our margin of heterogeneity is structural: the actors and their trait bundles are held fixed while the positions through which those traits enter the interaction are reassigned. The resulting question is how structural transmission changes the reduced dynamics and the accessibility of settlement.

Three results drive the paper. The first is analytical. A change of state and time scales reduces the vector-field geometry to four dimensionless combinations, making explicit which role–trait combinations alter feedback geometry and which alter scale. In particular, Role-3 leverage drops out of those four geometry groups and rescales the two principal coordinates. The second is dynamic. A stable settlement can coexist with a sustained irregular path, so equilibrium existence and practical access to that equilibrium are different questions. In one benchmark, reassigning the same three trait bundles raises the share of sampled opening positions that reach settlement from roughly 36% to more than 99%. The third is institutional. Reassignment moves a fixed trait multiset through reduced parameter space and changes settlement, periodic, chaotic, and coexistence outcomes; the effect survives a family of local perturbations to the nonlinear channels.

The empirical layer connects these abstract positions to observed three-party conflicts. In the Phoenix application, Roles 1 and 2 are occupied by government actors in a bilateral state dispute, while composite UNO supplies the third-party position. Historical event data reconstruct the three structural positions and rank their occupants on leverage, moderation, and vulnerability signals. A declared rank map places those ordinal signals on the benchmark model scale, while ICB and Near Crisis provide external checks on their economic interpretation. Phoenix supplies the role reconstruction and ordinal trait placement; the theoretical model supplies the continuous dynamics and the contrasting scenario environments.

The contribution is consequently about coordination through structure. In heterogeneous-agent models, changing the agents changes the interaction. Here the actors can remain fixed while the positions through which their traits are transmitted change the feedback itself. That mechanism affects both the long-run outcomes available to the bargaining process and the breadth of opening positions from which settlement can be reached. Section 2 develops the role architecture and local revision game, Section 3 gives the analytical results, Sections 4–5 report the numerical evidence, Section 6 reconstructs roles and trait rankings from historical data, and Section 7 returns to the economic implications.

## 2 Role-mediated adjustment model

Return to the wage negotiation. Suppose the firm makes the opening proposal, the union occupies the responding principal position, and public intervention is triggered by the state of their dispute. In this illustration the three participants instantiate the three structural positions. Elsewhere the same positions can be occupied by different actors; the model tracks how each trait bundle is transmitted once it enters a role.

An opening configuration is the vector of stances from which adjustment begins. Each coordinate records a signed displacement from that participant's own reservation benchmark. A stationary fixed point is a settlement configuration in the sense that local incentives to revise have disappeared. The model therefore follows the bargaining process up to a self-sustaining stance configuration. A terminal allocation rule can then attach wages, surplus shares, or other contractual terms to that settled state.

## 2.1 Structural roles in the bargaining process

The distinction between actor traits and structural positions is economically substantive. Proposal and recognition rules create initiating positions (Baron and Ferejohn 1989); network position affects bargaining power (Manea 2011; Abreu and Manea 2012); coercive capability changes the response available to a counterpart (Powell 1996); and mediation depends on the configuration of the disputants and the mode of intervention (Kydd 2003; Greig 2005; Rauchhaus 2006; Beardsley et al. 2006).

**Role 1 (initiator).** The initiating principal. Its stance responds directly to the counterpart, is pulled back by its own moderation, and is exposed to the third-party state through a vulnerability-mediated channel. Proposal and first-move rights make initiation an economically meaningful structural position (Baron and Ferejohn 1989; Galinsky and Mussweiler 2001).

**Role 2 (coercive counterpart).** The responding principal. It reacts directly to Role 1 and transmits leverage through a channel that depends on the joint Role-1/Role-3 configuration. This gives coercive capacity a different route into adjustment from ordinary persistence or moderation (Powell 1996; Anbarci et al. 2002).

**Role 3 (structurally reactive third party).** A third position activated by the joint configuration of the principals. Reactive denotes conditional activation by the principal configuration. Once activated, Role 3 changes its own stance and feeds back into both principals; its leverage therefore matters through an active response channel. This structure is consistent with evidence that third-party intervention depends on disputant information, resolve, and interaction conditions, and that third parties can alter conflict incentives while remaining strategic actors themselves (Kydd 2003; Rauchhaus 2006; Greig 2005; Halevy and Halali 2015).

The baseline architecture imposes three economic mechanisms. Own-state moderation creates self-damping pressure. The two principals respond directly to one another, so bilateral movement can reinforce further movement. The third role enters conditionally, only through the state of the principal interaction. Structural asymmetry then determines which trait component scales each channel. For parsimony, the baseline keeps the lowest polynomial order that represents those mechanisms: linear own-state terms, bilinear cross-role interactions, and the first triadic product. The sensitivity analysis later perturbs both the strength and form of these nonlinear channels.

The direct principal channel is reinforcing: $p, q > 0$ produce strategic complementarity in that component of local stance revision. Because $x_1$ and $x_2$ are departures from different reservation benchmarks, the same reinforcing channel can describe reciprocal hardening or reciprocal accommodation across the two positions. Conditional third-party feedback can then strengthen or offset that bilateral response away from the reference configuration.

The role-permutation experiment uses these positions literally: fixed trait bundles are moved across the three transmission rules while the rules themselves stay fixed. Empirical actor identities remain attached to the historical reconstruction; the counterfactual concerns structural assignment.

**Table 1** Role-specific channels. All leverage contributions are state-dependent; Role 2 carries a countervailing sign on the $x_1x_3$ interaction.

| **Role** | $L_i$ (leverage) | $M_i$ (moderation) | $V_i$ (vulnerability) | $F_i$ (forcing) |
|---|---|---|---|---|
| Role 1 (initiator) | $\alpha x_2$ | $-\alpha x_1$ | $-\gamma x_1 - x_1x_3$ | 0 |
| Role 2 (coercive counterpart) | $-x_1x_3$ | $-x_2$ | $-(1+\gamma)x_2$ | $\beta x_1$ |
| Role 3 (structurally reactive third party) | $x_1x_2$ | $-x_3$ | $-\gamma x_3$ | 0 |

## 2.2 States, traits, and role-specific channels

Let $x(t) = (x_1(t), x_2(t), x_3(t))^\top \in \mathbb{R}^3$. Each $x_i$ is a dimensionless signed bargaining-stance coordinate relative to actor $i$'s own reservation benchmark. In the opening illustration, $x_1$ and $x_2$ can be read as the firm's and union's current departures from the positions they are prepared to sustain, while $x_3$ records the mediator's intervention stance relative to its institutional benchmark. The same interpretation carries to any triad: magnitude measures positional displacement, while welfare and surplus shares belong to the bargaining outcome attached to the settled state.

Actor $i$ has self-moderation $C_i$, leverage $B_i$, and vulnerability $Y_i$. These characteristics travel with the actor when roles are reassigned. The contextual coefficients describe the bargaining environment: $\alpha > 0$ governs how strongly the Role-1 position transmits moderation and leverage, $\beta > 0$ scales Role-2 direct response, and $\gamma > 0$ governs how strongly vulnerability contributes to dissipation and exposure. Proposal rules, coercive context, mediation conditions, and time pressure provide economic reasons for allowing that transmission strength to vary across environments (Baron and Ferejohn 1989; Powell 1996; Rauchhaus 2006; Karagözoğlu and Kocher 2019).

Before introducing continuous time, write actor $i$'s local revision incentive as

$$f_i(x) = B_iL_i(x) + C_iM_i(x) + Y_iV_i(x) + F_i(x), \tag{1}$$

where $L_i$, $M_i$, and $V_i$ are the leverage, moderation, and vulnerability channels and $F_i$ is role-specific forcing independent of actor $i$'s own traits. Table 1 translates the three structural roles into these marginal incentives.

Equation (1) uses the convention $+Y_iV_i(x)$, so the dissipative signs sit inside the vulnerability kernels. For Role 2, for example, $V_2(x) = -(1+\gamma)x_2$: vulnerability contributes both its baseline damping and the environment-scaled term $-\gamma Y_2x_2$.

## 2.3 Local strategic stance revision

The channel structure becomes a bargaining process through repeated local revisions. Fix a short revision interval $\Delta > 0$. From current stance $x$, all three actors

simultaneously choose proposed next stances $z$. Actor $i$ solves

$$\max_{z_i} \left\{ \Pi_i(z_i, z_{-i}) - \frac{(z_i - x_i)^2}{2\Delta} \right\}. \tag{2}$$

The first term captures the bargaining incentive associated with the proposed configuration. The quadratic term captures the cost of moving too abruptly. Credibility, internal authorization, coalition commitments, and information revealed by a sudden concession all give such short-horizon adjustment costs an economic interpretation (Lucas 1967; Friedman and Ostrov 2010).

We choose the payoff representation so that actor $i$'s own-action marginal incentive is the role-specific field in Table 1, $\partial_{z_i}\Pi_i(z) = f_i(z)$. The simultaneous first-order conditions are therefore

$$z - x = \Delta f(z). \tag{3}$$

For sufficiently small $\Delta$, the implicit-function theorem gives a locally unique Nash revision near the current stance,

$$z(x, \Delta) = x + \Delta f(x) + O(\Delta^2). \tag{4}$$

As revision opportunities become frequent, the bargaining process converges to

$$\dot{x} = f(x). \tag{5}$$

Equations (2)–(5) give the strategic bridge from a discrete local revision problem to continuous stance adjustment. The formal local-uniqueness and concavity conditions are collected in Supplementary Section S1.

## 2.4 Role-mediated continuous-time dynamics

For compact notation define

$$A = \alpha C_1 + \gamma Y_1, \qquad D = C_2 + (1+\gamma) Y_2, \qquad E = C_3 + \gamma Y_3, \qquad p = \alpha B_1, \qquad q = \beta. \tag{6}$$

One convenient payoff representation consistent with Table 1 is

$$\begin{aligned} \Pi_1(z) &= p z_1 z_2 - \frac{A}{2} z_1^2 - \frac{Y_1}{2} z_1^2 z_3, \\ \Pi_2(z) &= q z_1 z_2 - \frac{D}{2} z_2^2 - B_2 z_1 z_2 z_3, \\ \Pi_3(z) &= B_3 z_1 z_2 z_3 - \frac{E}{2} z_3^2. \end{aligned} \tag{7}$$

Taking each actor's own-action marginal payoff and applying the frequent-revision limit yields

$$\dot{x}_1 = p x_2 - A x_1 - Y_1 x_1 x_3 \tag{8}$$

$$\dot{x}_2 = qx_1 - Dx_2 - B_2x_1x_3 \tag{9}$$
$$\dot{x}_3 = B_3x_1x_2 - Ex_3. \tag{10}$$

The first two equations combine reciprocal principal response with own-state damping and configuration-dependent third-party feedback. The third role activates through the joint principal configuration $x_1x_2$. Structural position therefore determines which part of an actor's fixed trait bundle enters direct response, conditional leverage, dissipation, or state scale.

We use the leverage-to-vulnerability ratio (LVR) as an ex-ante posture index,

$$\Phi_i = \frac{B_i}{Y_i}. \tag{11}$$

It summarizes coercive potential relative to vulnerability. Its realized effect remains role- and state-dependent.

# 3 Analytical properties

## 3.1 Equilibria and local geometry

The vector field is polynomial and locally Lipschitz. Its divergence is

$$\nabla \cdot F(x) = -(A + D + E) - Y_1x_3. \tag{12}$$

Local volume expansion is therefore possible when $x_3$ is sufficiently negative, even though Theorem 1 below keeps every forward trajectory globally bounded.

The origin is locally asymptotically stable exactly when

$$pq < AD. \tag{13}$$

When $pq > AD$, the origin is unstable and a symmetric pair of nonzero equilibria exists. The equality $pq = AD$ is the local stability boundary. The exact equilibrium coordinates and Jacobian identities are reported in Supplementary Section S1.

The two nonzero equilibria are related by the symmetry $(x_1, x_2, x_3) \mapsto (-x_1, -x_2, x_3)$. Depending on the parameter profile, they are either locally stable foci or saddle-foci with an unstable complex pair. This local geometry is important, but it does not by itself determine which long-run path is selected from a particular opening configuration.

## 3.2 Dimensionless structure and role-specific transmission

The twelve primitive actor/environment coefficients collapse to four combinations that govern vector-field geometry. With

$$\tau = Et, \qquad x_1 = s_1u, \qquad x_2 = s_2v, \qquad x_3 = s_3w, \tag{14}$$

**Table 2** Composite coefficients and their economic interpretation.

| Symbol | Definition | Plain meaning | Role's key channel |
|---|---|---|---|
| $A$ | $\alpha C_1 + \gamma Y_1$ | Role 1's effective dissipation | direct: $p\,x_2$ |
| $D$ | $C_2 + (1+\gamma)Y_2$ | Role 2's effective dissipation | direct: $q\,x_1$; conditional: $-B_2 x_1 x_3$ |
| $E$ | $C_3 + \gamma Y_3$ | Role 3's effective dissipation | conditional only: $B_3 x_1 x_2$ |
| $p$ | $\alpha B_1$ | Role 1 direct-response strength | — |
| $q$ | $\beta$ | Role 2 direct-response strength | — |

and scales $s_3 = E/Y_1$, $s_2/s_1 = E/p$, and $s_1^2 = pE/(Y_1 B_3)$, the model becomes

$$\begin{aligned} \frac{du}{d\tau} &= v - \delta_1 u - uw, \\ \frac{dv}{d\tau} &= \rho u - \delta_2 v - \chi uw, \\ \frac{dw}{d\tau} &= uv - w, \end{aligned} \tag{15}$$

where

$$\delta_1 = \frac{A}{E}, \qquad \delta_2 = \frac{D}{E}, \qquad \rho = \frac{pq}{E^2}, \qquad \chi = \frac{B_2 p}{Y_1 E}. \tag{16}$$

**Proposition 1 (four-group reduction).** Under the scaling in Equation (14), the reduced dynamics in Equation (15) depend only on the four groups in Equation (16). The origin condition becomes $\rho < \delta_1 \delta_2$.

These groups also have direct economic meaning. $\delta_1$ and $\delta_2$ compare principal-role dissipation with the Role-3 time scale. $\rho$ measures reciprocal principal reinforcement, and $\chi$ measures the Role-2 conditional-leverage channel relative to Role-1 vulnerability and Role-3 dissipation. Reassigning a fixed trait bundle changes these combinations because the same characteristic enters a different transmission rule.

The reduction exposes one exact asymmetry. Role-1 and Role-2 leverage enter the reduced geometry, whereas Role-3 leverage $B_3$ is absorbed into the scale of the two principal coordinates. Changing $B_3$ alone therefore rescales $(x_1, x_2)$ by a square-root factor while leaving the reduced vector field unchanged. A fixed physical opening state is nevertheless embedded at a different point in reduced coordinates, which matters when several attractors coexist. The exact conjugacy and reduced equilibrium formulas are given in the Online Supplement.

The reduced principal linear block has off-diagonal product $a_{12}a_{21} = \rho > 0$, the Lorenz-side sign in the Čelikovský and Chen (2002, 2005) classification of generalized Lorenz systems. We use that comparison to locate the dynamical architecture; the economic results below concern how structural roles move fixed actor characteristics through the reduced geometry and alter settlement accessibility.

### 3.3 Global boundedness

The long-run analysis requires the stance process to remain finite. The following result gives that guarantee; Supplementary Section S1 contains the complete Lyapunov construction.

**Theorem 1 (global boundedness).** Assume $C_i \geq 0$, $B_i > 0$, and $Y_i > 0$ for all $i$, together with $\alpha, \beta, \gamma > 0$. Then the flow defined by Equations (8)–(10) possesses a compact absorbing set. Every forward solution exists for all $t \geq 0$ and remains bounded.

The proof uses a shifted quadratic Lyapunov function with an $x_1 x_2$ cross term. That coupling tilts the level sets in the two-principal plane so that the cubic interactions cancel after shifting the Role-3 coordinate, leaving a negative quadratic drift outside a bounded region. Thus irregular bargaining paths can persist without the state variables diverging. All benchmark and role-permutation profiles satisfy the theorem's assumptions.

## 4 Numerical design

The numerical work asks two questions: which long-run path is selected from a given opening configuration, and how robustly a stable settlement can be reached when that opening is uncertain. Full solver settings, cross-solver checks, recurrence diagnostics, and machine-readable outputs are reported in the Online Supplement.

### 4.1 Long-run classification

All benchmark calculations use the common opening configuration $x(0) = (0.6, -0.3, 0.8)$ unless an opening-state distribution is stated explicitly. Set A is the contraction reference, so its asymptotic spectrum is obtained exactly from the stable-origin Jacobian. For B–E and the 24 heterogeneous role assignments, the authoritative classification uses a 10,000-unit warm-up followed by a 50,000-unit Lyapunov measurement window. Chaos requires agreement among a positive leading exponent, the neutral flow exponent, transverse contraction, solver checks, and nonperiodic recurrence. Periodic candidates are verified with root-located Poincar
'e crossings.

The role-sensitivity campaign evaluates all six assignments of B–E under the baseline and 12 local perturbations of the nonlinear channels, for 312 systems in total. Stable-focus cases whose common opening remains active receive an additional long persistence check. These calculations test whether the role effect survives small changes in channel strength and form rather than only the exact baseline algebra.

### 4.2 Settlement accessibility

A stable settlement may exist without being easy to reach. Let $T_S(x_0)$ be the first time an opening state enters the declared settlement neighborhood, and let $\mu$ describe uncertainty over opening configurations. For a horizon $H$ define

$$\mathcal{A}_\mu(H) = \mu\{x_0 : T_S(x_0) \leq H\}. \tag{17}$$

**Table 3** Baseline profiles in the reduced coordinates of Proposition 1. For Set A, $\lambda_1$ is the exact asymptotic Jacobian exponent at the stable origin. For B–E, $\lambda_1$ uses the 10,000/50,000 long-run protocol. Full spectra, primitive parameter vectors, and equilibrium coordinates appear in the Online Supplement.

| **Set** | $\delta_1$ | $\delta_2$ | $\rho$ | $\chi$ | $\lambda_1$ | **Regime from common opening** |
|---|---|---|---|---|---|---|
| A | 0.688 | 1.500 | 0.188 | 0.063 | −0.400 | settlement |
| B | 0.654 | 0.769 | 70.30 | 37.38 | 0.321 | chaotic |
| C | 0.636 | 0.743 | 137.76 | 34.33 | 0.417 | chaotic |
| D | 6.745 | 0.909 | 337.67 | 52.36 | 0.107 | settlement focus + chaotic path |
| E | 0.825 | 1.120 | 251.88 | 62.00 | 0.165 | chaotic |

Within the model, $\mathcal{A}_\mu(H)$ is the ex-ante likelihood that an uncertain opening reaches settlement within $H$ model-time units.

We estimate this quantity for every system with a locally stable nonzero focus, using four normalized focus-centered uncertainty ranges and a 20,000-unit horizon. Adaptive Monte Carlo sampling continues until the Wilson 95

# 5 Results

## 5.1 Benchmark regimes

Set A contracts to the stable origin. Sets B, C, and E generate bounded chaotic motion around unstable saddle-foci. Set D is different: its nonzero foci are locally stable, yet the common opening configuration reaches a distinct chaotic attractor. Set D also has the lowest long-run Kaplan–Yorke dimension (2.026; C 2.089; B/E 2.108), consistent with its comparatively compact attractor. Table 3 summarizes the benchmark regimes; full spectra and validation diagnostics are reported in the Online Supplement.

## 5.2 When a stable settlement is hard to reach

Set D is the clearest coordination problem in the benchmark set. The parameter environment contains two locally stable settlement foci, but it also supports a distinct sustained chaotic path. Open close enough to either settlement and revisions damp out. Start instead from the common opening configuration $x(0) = (0.6, -0.3, 0.8)$ and the same rules generate bounded irregular repositioning with long-run spectrum approximately $(0.107, 0.000, -4.063)$. State-only checks at $dt = 0.02$ and 0.005 show no settlement capture from that opening through $10^6$ model-time units.

Varying Role-2 posture while holding the opening state fixed reveals a sharp change in destination but an irregular time to settlement. On the declared grid the boundary lies between $\Phi_2 = 6.14210$ and 6.14215. Just below it, some trajectories settle quickly while nearby ones wander irregularly for thousands of model-time units; just above it, the common opening remains on the active path over the full observation horizon. Longer integrations at $\Phi_2 = 6.1425$ and 6.143 remain uncaptured through $10^6$ time units, even though the settlement focus is still locally stable. The complete scan and step-size checks are reported in the Online Supplement.

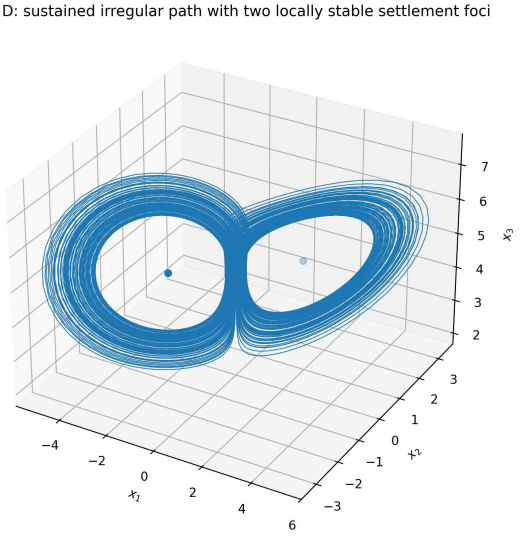



**Fig. 1** Set D from the common opening configuration after removal of the initial transient. The trajectory traces a bounded irregular path while the two marked nonzero equilibria are locally stable settlement foci.

The Monte Carlo experiment asks how forgiving each architecture is to uncertainty about the opening positions. The contrast is large even among systems that all contain a locally stable settlement. At the broadest reported uncertainty range, Set D settles from only about one-third of sampled openings, whereas the role-created B/(3,2,1) coexistence case settles from more than four-fifths; D/(1,3,2), whose alternative path is periodic, is accessible from almost all sampled openings. Thus the economic distinction is not simply whether a stable bargain exists, but how much of the plausible opening region can reach it. Exact fractions and confidence intervals are reported in Figure 2 and the Online Supplement.

## 5.3 Role-3 leverage, state scale, and reduced geometry

Role 3 is structurally reactive: $x_3$ is generated by the joint principal configuration and feeds back through both principal equations. Its leverage coefficient $B_3$ is absent from the four reduced geometry groups. Holding the remaining coefficients fixed, changing $B_3$ rescales $x_1$ and $x_2$ through the exact square-root conjugacy in Section 3.2, while $x_3$ is unchanged.

The asymmetry is economically sharp. Leverage carried by either principal changes the reduced feedback geometry, but the same leverage component assigned to Role 3 changes principal-state scale instead. Role 3 moderation and vulnerability still affect the reduced geometry through its dissipation term. Structural position therefore decides which part of the same trait bundle becomes regime-forming and which becomes scale-forming.

For a fixed physical opening state, a change in $B_3$ also changes the corresponding location in reduced coordinates. This matters whenever more than one attractor

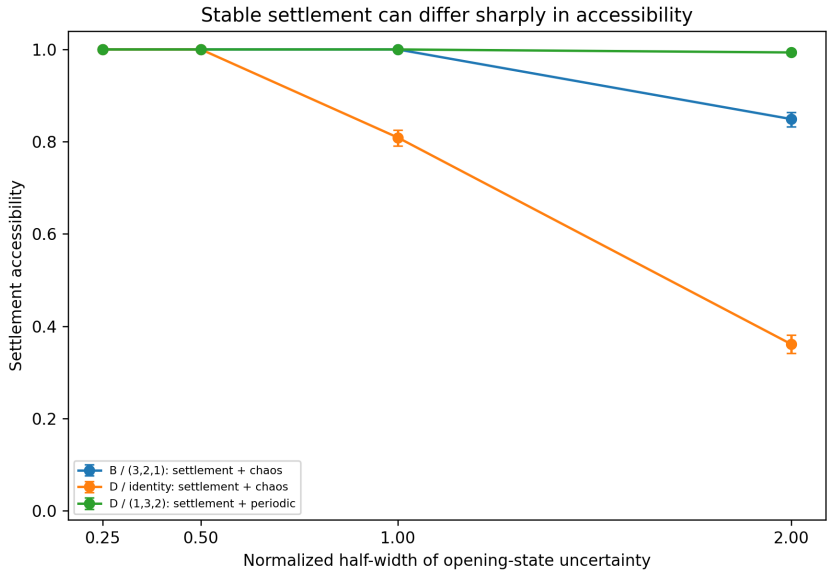



**Fig. 2** Settlement accessibility under normalized opening-state uncertainty for three baseline coexistence cases. Each point is the fraction of Monte Carlo openings captured by either stable settlement focus within the declared horizon; bars are Wilson 95% intervals. The same qualitative statement – a stable settlement exists alongside another sustained path – can therefore correspond to very different degrees of settlement accessibility.

is available: the conjugacy fixes the reduced vector field while relocating the same numerical opening configuration within reduced-coordinate basin geometry.

## 5.4 Changing roles without changing actors

The role-permutation experiment holds the three actor trait vectors $\theta_i = (C_i, B_i, Y_i)$ fixed within each profile and evaluates all six assignments to the structural positions. Environmental parameters, transmission rules, and the role-coordinate opening state are unchanged. The counterfactual reassigns trait bundles across response kernels; institutional identity and mandate stay in the empirical data layer.

Every heterogeneous profile spans more than one long-run architecture under reassignment. Figure 3 shows how a fixed trait multiset moves through the reduced space when the actors change structural positions. The plotted $(\delta_1, \chi)$ coordinates organize the cases but do not classify them: B/(1,3,2) and C/(1,3,2), for example, lie close together in this projection yet reach settlement and chaos because they differ strongly in the omitted reinforcement coordinate $\rho$. The destination therefore depends on the full reduced geometry and, where attractors coexist, on basin structure as well.

The same point appears in the two coexistence cases B/(3,2,1) and D/identity. Both contain a stable settlement focus alongside chaos and occupy a similar part of the plotted reduced space, yet their settlement accessibility is very different. A common attractor label can therefore hide economically important differences in how readily settlement is reached.

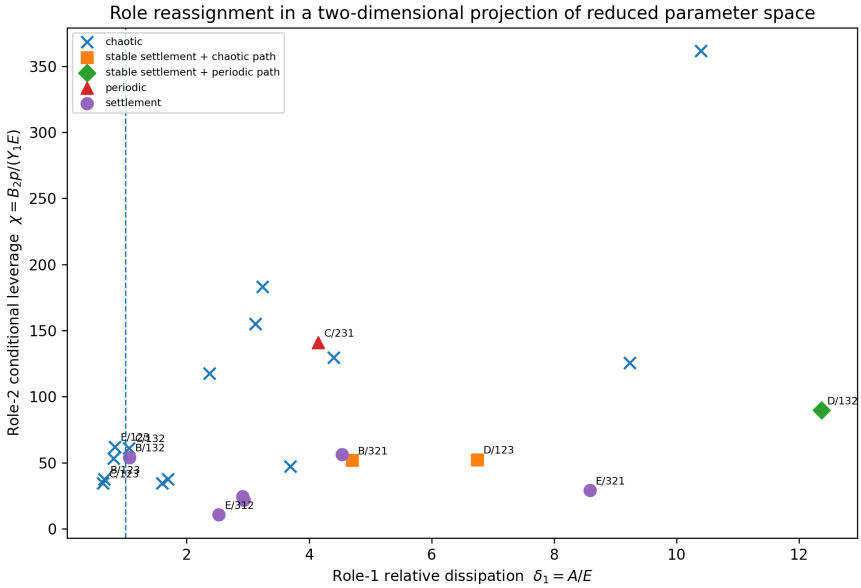



**Fig. 3** The 24 heterogeneous role assignments projected onto $(\delta_1, \chi)$, two of the four exact reduced coordinates. Marker type records attractor architecture. The nearby B/(1,3,2) and C/(1,3,2) points reach opposite regimes because the projection suppresses their large difference in $\rho$; the figure is therefore an organizing projection of the full reduced space.

**Table 4** Selected baseline role assignments in reduced coordinates. Accessibility is reported at normalized opening-state half-width $R = 2$ when a locally stable nonzero settlement focus exists. Complete 24-assignment results and the 312-case sensitivity analysis appears in the Online Supplement.

| Profile | Assign. | $\delta_1$ | $\chi$ | $\lambda_1$ | Access. | Attractor architecture |
|---|---|---|---|---|---|---|
| B | identity | 0.654 | 37.38 | 0.321 | – | chaotic |
| B | (3,2,1) | 4.700 | 51.84 | 0.084 | 0.849 | settlement focus + chaos |
| C | (2,3,1) | 4.148 | 140.92 | $\approx 0$ | – | periodic |
| D | identity | 6.745 | 52.36 | 0.107 | 0.361 | settlement focus + chaos |
| D | (1,3,2) | 12.367 | 89.60 | $\approx 0$ | 0.994 | settlement focus + periodic |
| D | (2,3,1) | 2.373 | 117.60 | 0.252 | – | chaotic |
| E | (3,1,2) | 2.525 | 10.64 | $-0.134$ | 1.000 | settlement |

The local channel-sensitivity analysis separates two robustness questions. Looking only at the path from the common opening state, role-induced regime diversity survives all 13 tested architectures for B, C, and E and 10 of 13 for D. Looking at the full attractor architecture, including the presence of a stable settlement focus alongside the active path, role assignment changes the architecture in all 13 tested variants for every B–E profile. The exact orbit labels are more sensitive than the broader role effect.

### 5.5 What the long-run paths mean for bargaining

The dynamical labels describe different bargaining processes. Settlement means that the incentive to revise has died out and the stance configuration sustains itself. Periodic motion means that repositioning continues but becomes recurrent: hardening, accommodation, and third-party response repeat in an ordered sequence. Chaotic motion is different again. Revisions remain bounded, yet the feedback among the roles keeps recreating new incentives to move, so the path stays irregular even though the actors and institutional parameters are fixed.

Set D is the mathematical version of the contrast in the opening wage negotiation. One set of opening positions falls into a self-damping region and reaches the stable bargain. Another activates feedback that keeps the principals and third party repositioning. The parameter scan around $\Phi_2 \simeq 6.142$ changes the thought experiment: the opening state is held fixed while Role-2 posture changes slightly. The destination boundary is sharp on the declared grid, but the time required to settle below it becomes highly irregular. In economic terms, the architecture can make both the destination and the delay to agreement sensitive to small changes in the bargaining environment.

The role-permutation results add the institutional margin. The firm, union, and mediator in the illustration are only one possible assignment of actors to positions. Moving a fixed trait bundle to another structural role changes the feedback gains and the opening state's location in basin geometry. The same participants can therefore face a different degree of settlement accessibility even when their underlying characteristics are unchanged.

## 6 Empirical role reconstruction and trait anchoring

The empirical layer has two jobs: reconstruct the structural positions observed in historical bargaining episodes and place actor traits in ordinal relation to one another. Historical Phoenix records provide dated directed interactions and CAMEO action codes at calendar-day resolution. Event order is used to assign the principal roles, while date incidence and response sequences produce leverage, moderation, and vulnerability rankings. Those rankings are then mapped monotonically to the model's declared trait scale. The contextual coefficients $\alpha$, $\beta$, and $\gamma$ remain scenario parameters describing the bargaining environment. ICB and Near Crisis are used separately to check whether the three trait labels behave in the expected economic direction.

### 6.1 Phoenix candidate trajectories and structural roles

We use the Cline Center Historical Phoenix Event Data, v1.3.0 (Althaus et al. 2020), combining the BBC Summary of World Broadcasts (SWB, 1979–2019) and Foreign Broadcast Information Service (FBIS, 1995–2004) event files. The two files contain 5,073,710 source rows. We retain directed events with identified and distinct source and target actors, group them by unordered principal dyad, and order each dyad chronologically. CAMEO is hierarchical: throughout, *root* denotes the two-digit top-level event category, while codes such as 057 and 0874 are lower-level event codes (Schrodt 2012). CAMEO 057 (sign formal agreement) and 0874 (retreat or surrender

**Table 5** Phoenix reconstruction and response-depth counts.

| Stage | Count |
|---|---|
| Original SWB+FBIS event rows | 5,073,710 |
| Bilateral timelines generating candidate trajectories | 8,176 |
| Candidate trajectories | 34,682 |
| Resolved Role-1/Role-2 trajectories | 22,441 |
| Clean complete Role-1/Role-2/composite-UNO trajectories | 17,010 |
| All roles: minimum response count 5 (sensitivity population) | 1,099 |
| All roles: minimum response count 10 (primary anchoring population) | 446 |

militarily) define trajectory boundaries; 0871 (declare truce/ceasefire) is kept within the ongoing trajectory. This procedure yields 34,682 reconstructed candidate trajectories from 8,176 bilateral timelines. The construction is mechanical and identical across dyads; full screening and boundary rules appear in the Online Supplement.

In the Phoenix reconstruction, both principal positions are occupied by government actors. Composite UNO is the third-party actor. Role assignment is constructed separately from the trait measures. Within each government dyad, the source of the earliest unilateral root-10 demand becomes Role 1 and the other government principal becomes Role 2. When no unilateral first demand resolves the pair, Role 1 is assigned to the principal whose first outgoing action occurs nearest the trajectory's first active date. Phoenix calendar-day resolution resolves event order up to same-day ties. This yields 22,441 resolved principal pairs.

Composite UNO provides the primary Phoenix realization of Role 3. We identify the endpoint when root `IGO` carries the exact `UNO` token in the same auxiliary actor-code field and the resulting composite actor interacts with both principals during the trajectory. Combined with resolved principal roles and non-generic principal identities, this rule yields 17,010 clean complete triads. The third-party relation is persistent rather than incidental: the median number of active dates with the less-contacted principal is 14, and 58.2% of qualified cases have at least ten active dates with each principal. Composite UNO is active as well, originating at least one root-10–20 pressure event in 81.31% of qualified trajectories; 21.45% contain explicit mediation-context evidence. The Online Supplement gives the full coding and persistence audit.

## 6.2 Actor-trait signals and numerical anchoring

Phoenix provides event-based measures for the three actor traits. For leverage, the broad-pressure family is CAMEO roots 10–20: Demand (10), Disapprove (11), Reject (12), Threaten (13), Protest (14), Exhibit Force Posture (15), Reduce Relations (16), Coerce (17), Assault (18), Fight (19), and Use Unconventional Mass Violence (20). The CAMEO codebook orders roots 10–20 as increasing in conflict (Schrodt 2012). Leverage is the share of outgoing-active dates containing at least one event from this family,

$$B_i^{\mathrm{P}} = \frac{\#\{\text{outgoing-active dates with root 10–20}\}}{\#\{\text{outgoing-active dates}\}}. \tag{18}$$

Moderation uses the corresponding incidence of roots 03–08, spanning Express Intent to Cooperate, Consult, Engage in Diplomatic Cooperation, Engage in Material Cooperation, Provide Aid, and Yield. Date incidence limits the influence of repeated same-day reporting. Vulnerability is measured through response behavior: following incoming broad pressure, the first strictly later outgoing-active date is paired as the response, and the probability of a broad-moderation response is compared with the corresponding probability following non-pressure incoming activity over a 90-day horizon. The resulting uplift is used as a vulnerability ranking.

Vulnerability requires enough observed responses to estimate the pressure-versus-non-pressure uplift. We therefore apply a response-depth requirement to each actor-role $Y$ estimate: the underlying first-next-response comparison must contain at least a declared minimum number of qualifying response observations. Across the 17,010 clean complete triads, all three roles have usable leverage/moderation signals in 16,849 cases. Requiring every role's 90-day $Y$ comparison to meet a minimum response count of 5 leaves 1,099 trajectories; raising that minimum to 10 leaves 446. We retain the 446 as the primary higher-response-depth anchoring population and use the broader 1,099 as a threshold-sensitivity population. The Online Supplement compares the two mappings directly and contrasts the 446 trajectories with the 653 additional cases admitted by the 5-observation requirement.

For the primary 446-trajectory anchoring population, pooling the three roles gives 1,338 observations for each trait. Average midranks are converted to percentiles,

$$p = \frac{\text{midrank} - 0.5}{1338}, \tag{19}$$

and mapped monotonically to the existing model scale,

$$B = 0.20 + 0.75p, \qquad C = 0.05 + 0.65p, \qquad Y = 0.02 + 0.58p. \tag{20}$$

Equations (19)–(20) use one pooled reference across all three roles, preserving empirical cross-role differences in ordering and relative level. Phoenix identifies the ordinal placement; the endpoint values provide the benchmark model's cardinal normalization. For the response-depth sensitivity check, the same procedure is recomputed independently on the 1,099 trajectories, giving 3,297 pooled actor-role values per trait while retaining the same cardinal endpoints. A logarithmic interpolation over the same endpoints provides a scaling-shape robustness check.

Phoenix ranks leverage and vulnerability separately, and Table 6 reports the resulting role-specific posture distributions at both response-depth thresholds. In the primary 446-trajectory mapping, the two principal roles have similar medians, $\Phi_1 = 2.25$ and $\Phi_2 = 2.22$, whereas the reactive third position has median $\Phi_3 = 1.25$ and a markedly shorter upper tail (95th percentile 6.28 versus 17.35 and 14.56 for Roles 1 and 2). Recomputing the mapping on all 1,099 trajectories preserves the same cross-role pattern: the medians are 2.29, 2.12, and 1.42, and the corresponding 95th percentiles are 14.89, 14.21, and 6.92. The broader population therefore reinforces the principal-versus-third-role contrast; the higher response-depth requirement sharpens rather than creates it. The cardinal map contributes an inherited scale asymmetry

**Table 6** Mapped leverage-to-vulnerability posture under the two response-depth thresholds. Each threshold is ranked within its own pooled actor-role reference and mapped to the same fixed trait envelopes. The interval is the empirical 5th–95th percentile range; coverage reports the share inside the benchmark posture range $[0.5, 20]$.

| Min. responses | Role | Median $\Phi$ | 5th–95th pct. | Coverage |
|---|---|---|---|---|
| 10 | Role 1 | 2.25 | $[0.61, 17.35]$ | 93.5% |
| 10 | Role 2 | 2.22 | $[0.71, 14.56]$ | 96.2% |
| 10 | Role 3 | 1.25 | $[0.44, 6.28]$ | 92.6% |
| 5 | Role 1 | 2.29 | $[0.67, 14.89]$ | 96.8% |
| 5 | Role 2 | 2.12 | $[0.60, 14.21]$ | 95.3% |
| 5 | Role 3 | 1.42 | $[0.49, 6.92]$ | 93.8% |

because the declared $Y$ envelope spans a larger proportional range than the $B$ envelope. Accordingly, the empirical comparison uses the cross-role posture distributions; within-role component correlations are shaped mechanically by the declared mapping.

The anchoring exercise inherits the measurement structure of the historical event record. SWB and FBIS contribute different periods and source systems; event incidence reflects reporting and coding as well as behavior; the broad root-10–20 leverage family pools heterogeneous pressure and coercion actions; open trajectories contribute right-censored histories; and negative vulnerability uplifts record a lower conciliatory response after incoming pressure and therefore occupy the low-vulnerability end of the pooled ranking. The empirical archive also retains a narrower hard-pressure construction for coding sensitivity. These features define the scope of the historical-event anchoring exercise.

## 6.3 External triangulation of trait interpretation

Two independent crisis datasets provide complementary checks on the trait interpretation. First, the International Crisis Behavior data use actor-level capability differential (`POWDIS`), crisis-management technique (`CRISMG`), and gravity of threat (`GRAVTY`) as proxies for leverage, moderation, and vulnerability. In the broad actor-crisis comparison, 77.3% of the implied leverage-to-vulnerability ratios lie inside the archetypal $[0.5, 20]$ range. Among confirmed bilateral crisis rows the corresponding coverage is 55.2%, reflecting a heavier upper tail of capability asymmetry. A ratio-form capability construction produces moderate rank agreement with the difference-form measure (Spearman $\rho = 0.29$), so the external comparison supports the broad interpretation while also showing that cardinal leverage depends on the conflict-technology representation. Full calculations are reported in the Online Supplement (Brecher and Wilkenfeld 1997; Brecher et al. 2025; Hewitt 2003; Hirshleifer 1989; Skaperdas 1996).

Second, the Near Crisis data use the same ICB coding protocol (Iakhnis and James 2019). Near-crisis actors display substantially higher moderation than crisis actors (mean 5.22 versus 3.10, Cohen's $d = 0.97$) and lower vulnerability (3.58 versus 4.21, $d = -0.42$). The direction of both differences matches the model's interpretation of those traits.

Phoenix supplies structural positions and actor-specific ordinal $B_i, C_i, Y_i$ information, while ICB and Near Crisis provide broad external interpretation checks. The environmental coefficients act as contextual scenario controls. Evidence that proposal rights, coercive power, third-party intervention, and time pressure alter bargaining response motivates this separation (Baron and Ferejohn 1989; Powell 1996; Rauchhaus 2006; Karagözoğlu and Kocher 2019); their numerical values define contrasting model environments on the normalized scale.

# 7 Discussion

## 7.1 Structural position as a coordination mechanism

The main result is easier to state economically than dynamically: the same actors can face different coordination problems when their characteristics are transmitted through different positions. Heterogeneous-agent models usually change what agents bring to an interaction (Brock and Hommes 1998; Hommes 2006). The role experiment holds the trait endowment fixed and changes the feedback architecture. Proposal rights, network position, coercive authority, and third-party design already matter in bargaining theory (Baron and Ferejohn 1989; Manea 2011; Abreu and Manea 2012; Beardsley et al. 2006); the present model shows one way in which those institutional differences can change the dynamics themselves.

Proposition 1 makes the mechanism visible. Role-1 leverage changes both bilateral reinforcement $\rho$ and conditional leverage $\chi$; Role-2 leverage enters $\chi$ directly. Role-3 leverage instead fixes principal-state scale, while Role-3 moderation and vulnerability enter the common dissipation scale $E$. Position therefore determines which part of a trait bundle changes feedback geometry and which part changes the scale on which the bargaining path is expressed.

The reduced-space figure also shows why no single ratio should be read as a threshold. B/(1,3,2) and C/(1,3,2) nearly coincide in the plotted $(\delta_1, \chi)$ projection and still reach opposite regimes because $\rho$ differs sharply. The full four-dimensional geometry matters, and coexistence adds basin structure on top of it.

## 7.2 Settlement accessibility and institutional design

A locally stable settlement answers a narrow question: if bargaining is already close to that configuration, will revisions return to it? Accessibility asks the institutional question that matters before the meeting begins. Given uncertainty over opening offers, demands, and third-party posture, how often does the process reach the stable bargain within the chosen horizon? Equation (17) makes that question explicit.

The coexistence cases show why the distinction matters. Set D and B/(3,2,1) both contain a stable focus and a chaotic attractor, yet at $R = 2$ their settlement accessibilities are about 0.36 and 0.85. D/(1,3,2) contains a stable focus and a periodic alternative but remains accessible from about 0.99 of the sampled openings. In the wage-negotiation analogy, all three institutional arrangements possess a viable agreement configuration; what differs is the size of the set of opening positions from which the parties can actually get there.

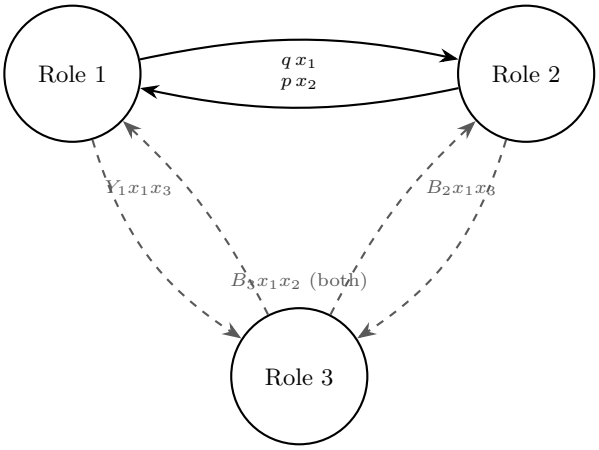



**Fig. 4** Role-interaction graph. Solid edges are direct linear dependencies; dashed edges are conditional dependencies through multiplicative cross-terms.

This is also where the paper connects most directly to coordination and dynamic selection. Structural assignment changes the feedback that acts on the same trait multiset. That changes both which long-run paths are available and how robustly settlement is selected when the opening configuration is uncertain. The role architecture therefore acts as an institutional selection mechanism by changing how a fixed trait multiset feeds back through the interaction.

The empirical reconstruction supports the first part of that mechanism: it identifies structural positions in historical event sequences and supplies ordinal information on actor traits. A natural next step is to connect the latent stance path to observed event sequences through an explicit observation model. Such a layer could estimate contextual transmission parameters and compare model-implied settlement timing or escalation patterns with historical trajectories. The current analysis establishes the structural mechanism and its consequences on the model's declared state and time scales.

# 8 Conclusion

The paper began with a simple bargaining puzzle: why can the same participants settle from one opening configuration and remain locked in repositioning from another? The model's answer is structural. Actor characteristics matter through the positions that transmit them. Changing those positions changes bilateral reinforcement, dissipation, conditional third-party feedback, and the basin geometry surrounding a stable settlement.

The four-group reduction gives this claim an exact analytical form. Role-1 and Role-2 leverage enter reduced geometry; Role-3 leverage sets principal-state scale. The numerical results then show what that asymmetry can do. Fixed trait bundles produce settlement, periodic adjustment, chaos, and coexistence under different assignments, and the broader role effect persists under local perturbations of the nonlinear channels.

The accessibility results give the multistability finding its economic bite. A stable bargain can exist and still be difficult to reach. In Set D, only about 0.36 of the broadest sampled opening distribution reaches settlement within the declared horizon, compared with about 0.85 in B/(3,2,1), even though both systems contain a stable settlement focus alongside chaos. The economic difference is how forgiving the interaction architecture is to where bargaining begins, even when both systems contain a stable agreement configuration.

Phoenix data anchor the structural positions and ordinal trait heterogeneity to historical interaction records, while ICB and Near Crisis support the economic interpretation of the trait dimensions. The resulting framework adds structural assignment to the usual sources of agent heterogeneity. That opens a further institutional question: when roles can be chosen or designed, bargaining institutions shape both who participates and the channels through which each participant's characteristics affect the path to agreement.

**Supplementary information.** An Online Supplement accompanies this article with the full boundedness proof, numerical protocols, benchmark and role-permutation tables, Phoenix reconstruction details and robustness checks.

## References


Althaus, S., Bajjalieh, J., Carter, J., Peyton, B., Shalmon, D.: Cline Center Historical Phoenix Event Data. Cline Center for Advanced Social Research, version 1.3.0, University of Illinois Urbana-Champaign (2020). https://doi.org/10.13012/B2IDB-0647142_V3

Agiza, H.N., Bischi, G.I., Kopel, M.: Multistability in a dynamic cournot game with three oligopolists. Math Comput Simul **51**(1–2), 63–90 (1999) https://doi.org/10.1016/S0378-4754(99)00106-8

Ambrus, A., Lu, S.E.: A continuous-time model of multilateral bargaining. Am Econ J Microecon **7**(1), 208–249 (2015) https://doi.org/10.1257/mic.20100029

Abreu, D., Manea, M.: Markov equilibria in a model of bargaining in networks. Games Econ Behav **75**(1), 1–16 (2012) https://doi.org/10.1016/j.geb.2011.09.002

Anbarci, N., Skaperdas, S., Syropoulos, C.: Comparing bargaining solutions in the shadow of conflict: How norms against threats can have real effects. J Econ Theory **106**(1), 1–16 (2002) https://doi.org/10.1006/jeth.2001.2893

Baron, D.P., Ferejohn, J.A.: Bargaining in legislatures. Am Polit Sci Rev **83**(4), 1181–1206 (1989) https://doi.org/10.2307/1961664

Brock, W.A., Hommes, C.H.: Heterogeneous beliefs and routes to chaos in a simple asset pricing model. J Econ Dyn Control **22**(8-9), 1235–1274 (1998) https://doi.org/10.1016/S0165-1889(98)00011-6

Bischi, G.I., Lamantia, F.: Evolutionary oligopoly games with cooperative and aggressive behaviors. J Econ Interact Coord **17**, 3–27 (2022) https://doi.org/10.1007/s11403-020-00298-y

Beardsley, K.C., Quinn, D.M., Biswas, B., Wilkenfeld, J.: Mediation style and crisis outcomes. J Confl Resolut **50**(1), 58–86 (2006) https://doi.org/10.1177/0022002705282862

Brecher, M., Wilkenfeld, J.: A Study of Crisis. University of Michigan Press, Ann Arbor, MI (1997)

Brecher, M., Wilkenfeld, J., Beardsley, K., James, P., Quinn, D.: International crisis behavior data codebook, version 16. Technical report, International Crisis Behavior Project (2025)

Filzmoser, M., Hippmann, P., Vetschera, R.: Analyzing the multiple dimensions of negotiation processes. Group Decis Negot **25**, 1169–1188 (2016) https://doi.org/10.1007/s10726-016-9477-7

Friedman, D., Ostrov, D.N.: Gradient dynamics in population games: Some basic results. J Math Econ **46**(5), 691–707 (2010) https://doi.org/10.1016/j.jmateco.2010.08.006

Galinsky, A.D., Mussweiler, T.: First offers as anchors: The role of perspective-taking and negotiator focus. J Pers Soc Psychol **81**(4), 657–669 (2001)

Greig, J.M.: Stepping into the fray: When do mediators mediate? Am J Polit Sci **49**(2), 249–266 (2005) https://doi.org/10.1111/j.0092-5853.2005.00121.x

Hewitt, J.J.: Dyadic-level international crisis data, version 2.0. Technical report, International Crisis Behavior Project (2003)

Halevy, N., Halali, E.: Selfish third parties act as peacemakers by transforming conflicts and promoting cooperation. Proc Natl Acad Sci USA **112**(22), 6937–6942 (2015) https://doi.org/10.1073/pnas.1505067112

Hirshleifer, J.: Conflict and rent-seeking success functions: Ratio vs. difference models of relative success. Public Choice **63**(2), 101–112 (1989) https://doi.org/10.1007/BF00153897

Hommes, C.H.: Heterogeneous agent models in economics and finance. In: Tesfatsion, L., Judd, K.L. (eds.) Handbook of Computational Economics, Vol. 2: Agent-Based Computational Economics, pp. 1109–1186. Elsevier, Amsterdam (2006). Chap. 23

Iakhnis, E., James, P.: Near crises in world politics: A new dataset. Confl Manag Peace Sci, 1–20 (2019) https://doi.org/10.1177/0738894219855610

Kaufman, M., Diep, H.T., Kaufman, S.: Sociophysics of intractable conflicts: Three-group dynamics. Physica A **517**, 175–187 (2019) https://doi.org/10.1016/j.physa.2018.11.003

Karagözoğlu, E., Kocher, M.G.: Bargaining under time pressure from deadlines. Exp Econ **22**, 419–440 (2019) https://doi.org/10.1007/s10683-018-9579-y

Kydd, A.: Which side are you on? bias, credibility, and mediation. Am J Polit Sci **47**(4), 597–611 (2003) https://doi.org/10.1111/1540-5907.00042

Lee, J., Liu, Q.: Gambling reputation: Repeated bargaining with outside options. Econometrica **81**(4), 1601–1672 (2013) https://doi.org/10.3982/ECTA9200

Lucas, R.E.: Adjustment costs and the theory of supply. J Polit Econ **75**(4), 321–334 (1967) https://doi.org/10.1086/259289

Manea, M.: Bargaining in stationary networks. Am Econ Rev **101**(5), 2042–2080 (2011) https://doi.org/10.1257/aer.101.5.2042

Naimzada, A.K., Tramontana, F.: Two different routes to complex dynamics in an heterogeneous triopoly game. J Differ Equ Appl **21**(7), 553–563 (2015) https://doi.org/10.1080/10236198.2015.1040403

Nikolova, E.V., Vitanov, N.K.: On the possibility of chaos in a generalized model of three interacting sectors. Entropy **22**(12), 1388 (2020) https://doi.org/10.3390/e22121388

Ortner, J.: A continuous-time model of bilateral bargaining. Games Econ Behav **113**, 720–733 (2019) https://doi.org/10.1016/j.geb.2018.12.001

Powell, R.: Bargaining in the shadow of power. Games Econ Behav **15**(2), 255–289 (1996) https://doi.org/10.1006/game.1996.0068

Rauchhaus, R.W.: Asymmetric information, mediation, and conflict management. World Polit **58**(2), 207–241 (2006) https://doi.org/10.1353/wp.2006.0027

Schrodt, P.A.: CAMEO: Conflict and Mediation Event Observations Event and Actor Codebook. Version 1.1b3, Event Data Project, Department of Political Science, Pennsylvania State University (2012). https://eventdata.parusanalytics.com/cameo.dir/CAMEO.Manual.1.1b3.pdf

Skaperdas, S.: Contest success functions. Econ Theory **7**(2), 283–290 (1996)

Čelikovský, S., Chen, G.: On a generalized lorenz canonical form of chaotic systems. Int J Bifurc Chaos **12**(8), 1789–1812 (2002) https://doi.org/10.1142/S0218127402005467

Čelikovský, S., Chen, G.: On the generalized lorenz canonical form. Chaos Solitons

Fractals **26**(5), 1271–1276 (2005) https://doi.org/10.1016/j.chaos.2005.02.040

## Supplementary Files

This is a list of supplementary files associated with this preprint. Click to download.

- SupplementGLLD.zip